Finite element modeling of seismic attenuation due to fluid flow in partially saturated rocks

Beatriz Quintal, ETH Zurich, Holger Steeb, Ruhr-University Bochum, Marcel Frehner, University of Vienna, and Stefan M. Schmalholz, ETH Zurich*

Summary

The finite element method is used to solve Biot's quasi-static equations of consolidation. We perform 1D and 2D numerical creep tests of partially saturated porous rocks to calculate the frequency-dependent seismic attenuation and phase velocity from the modeled stress-strain relations. The resulting attenuation and velocity dispersion are due to fluid flow induced by pressure differences between mesoscopic-scale regions of the rock fully saturated with different fluids (White's model). Comparisons of our numerical results with analytical solutions show accuracy for a wide range of frequencies. The algorithm is applied to a 1D partially saturated rock with a random distribution of saturation. We show that the numerical results for the random distribution can be approximated with a volume average of analytical solutions for periodic media.

Introduction

Attenuation of seismic waves in partially saturated rocks is of great interest because it has been observed that gas and oil reservoirs often exhibit high attenuation (e.g., Dasgupta and Clark, 1998; Rapoport et al., 2004), especially at low frequencies (Chapman et al., 2006). Data, from both laboratory and field, and theoretical work show that attenuation can be related to an increase in reflectivity in the low-frequency range (Korneev et al., 2004; Quintal et al., 2009). Goloshubin et al. (2006) showed three examples of field data in which oil-rich reservoirs exhibit increased reflectivity at low seismic frequencies (around 10 Hz).

At low seismic frequencies, wave-induced fluid flow on the mesoscopic scale is presumably the major cause of wave attenuation and velocity dispersion in partially saturated porous rocks (e.g., Norris, 1993; Johnson, 2001; Pride and Berryman, 2003a, b). The mesoscopic scale is the scale much larger than the pore size, but much smaller than the wavelength. White (1975) and White et al. (1975) were the first to introduce the wave-induced fluid flow mechanism for a 3D model of a water-saturated medium with spherical gas-saturated inclusions and a 1D layered model. In White's model, a partially saturated rock is represented by a poroelastic solid with regions fully saturated by one fluid and regions fully saturated by another fluid. Wave-induced fluid flow is caused by pore pressure differences between the two regions. Dutta and Odé (1979a, b) showed that wave-induced fluid flow can be modeled using Biot's equations (Biot, 1962) for wave propagation in poroelastic media with spatially varying petrophysical parameters. Several theoretical studies, based on White's model and Biot's theory (Biot, 1962), provide various closed-form analytical solutions for seismic attenuation in porous saturated media with periodic mesoscopic-scale heterogeneities of particular geometries, such as layered media or media with spherical inclusions (e.g., Johnson, 2001; Pride and Berryman, 2003a, b). There are also closed-form analytical solutions for randomly layered media (e.g., Gurevich and Lopatnikov, 1995), however, they are restricted to infinite media and to particular autocorrelation functions. Müller and Gurevich (2005) showed that significant differences in the magnitude and frequency dependence of attenuation are caused by only the use of different autocorrelation functions. Additionally, in the low-frequency limit, $1/Q$ (Q is the quality factor, $1/Q$ is a measure of attenuation) scales differently in infinite randomly layered media, compared to periodically layered media or finite randomly layered media. For infinite random media, $1/Q$ is proportional to the square root of frequency, while for periodic and finite random media it is proportional to frequency (Müller and Rothert, 2006).

Thus, stable and accurate numerical solutions for seismic attenuation in porous saturated media with mesoscopic-scale heterogeneities are required, for example, for: (i) heterogeneities with complicated geometries, (ii) finite random media with arbitrary distribution pattern, or (iii) media containing more than two heterogeneities, such as partial saturations with more than two fluids.

Calculating seismic attenuation due to wave-induced fluid flow with numerical algorithms for wave propagation in poroelastic media (e.g., Zhu and McMechan, 1991) is computationally inefficient because wave propagation, fluid flow and fluid pressure diffusion occur on different time scales. An efficient method is a quasi-static creep test, suggested by Masson and Pride (2007), in which they solved Biot's equations (Biot, 1962) for wave propagation in poroelastic media with the finite difference method. In this study, we performed similar quasi-static creep tests for calculating seismic attenuation as suggested by Masson and Pride (2007), however, we solved a simpler mathematical problem, Biot's equations of consolidation (Biot, 1941), in which inertia forces do not play a significant role and therefore are excluded. Attenuation due to wave-induced fluid flow is controlled by fluid pressure diffusion. For calculating the amount of attenuation, it is sufficient to model only the pressure diffusion. We used the finite element method to solve Biot's equations of consolidation in the u-p formulation (Zienkiewicz and Shiomi, 1984). We show that our numerical scheme is powerful and accurate in calculating attenuation and velocity dispersion due to the

wave-induced fluid flow mechanism. We further show that averages of White's analytical solution provide a good estimate for attenuation and velocity dispersion in rocks with random distributions of saturation.

The u-p formulation of Biot's equations of consolidation

Biot's equations of consolidation (Biot, 1941) are

$$\begin{aligned} -\nabla\cdot\boldsymbol{\sigma} &= 0, \\ -\nabla\cdot\left(\frac{k}{\eta}\nabla p\right) + \alpha\nabla\cdot\dot{\boldsymbol{u}} + \frac{\dot{p}}{M} &= 0, \end{aligned} \tag{1}$$

where a dot on top of a variable represents the first time derivative and ∇ is the Nabla operator for spatial derivatives. Material parameters are defined in Table 1. The symbol p denotes the pore fluid pressure, $\boldsymbol{u}$ is the vector of solid displacements with components u_i in the i-th directions, and $\boldsymbol{\sigma}$ is the total stress tensor with components

$$\sigma_{ij} = 2\mu\varepsilon_{ij} + \lambda e\delta_{ij} - \alpha p\delta_{ij} \tag{2}$$

(Biot, 1941; Biot, 1962), where δ_{ij} is the Kronecker delta. The components of the strain tensor are

$$\varepsilon_{ij} = \frac{1}{2}\left(\frac{\partial u_i}{\partial x_j} + \frac{\partial u_j}{\partial x_i}\right) \tag{3}$$

and the cubical dilatation is

$$e = \sum_{i=1}^{n}\varepsilon_{ii}\,. \tag{4}$$

Using equation 2, equations 1 can be expressed in terms of the two unknowns $\boldsymbol{u}$ and p, therefore called u-p formulation (e.g. Zienkiewicz and Shiomi, 1984).

Table 1. Definitions of symbols for the petrophysical parameters.

Symbol	Petrophysical parameter
k	Permeability
η	Viscosity of the fluid
Φ	Porosity
μ	Shear modulus of the dry frame
K	Bulk modulus of the dry frame
K_s	Bulk modulus of the solid grains
K_f	Bulk modulus of the fluid
ρ_s	Density of the solid grains
ρ_f	Density of the fluid
λ	$K - 2\mu/3$
α	$1 - K/K_s$
M	$1/(\Phi/K_f - (\alpha - \Phi)/K_s)$

The finite element scheme

Biot's equations of consolidation in the u-p formulation are solved with the finite element method, using the Galerkin method (Zienkiewicz and Taylor, 1989). Due to the u-p formulation, our scheme benefits from natural boundary conditions for fluid flow and prescribed total stresses. We use a first order implicit finite difference operator for the time derivative. For the 2D scheme, an unstructured triangular numerical mesh (Shewchuk, 1996, 2002) is used in a way that material boundaries coincide with element boundaries, allowing a spatially variable resolution, as shown in Figure 1 (Frehner et al., 2008). The element is triangular and isoparametric with seven nodes (Zienkiewicz and Taylor, 1989).

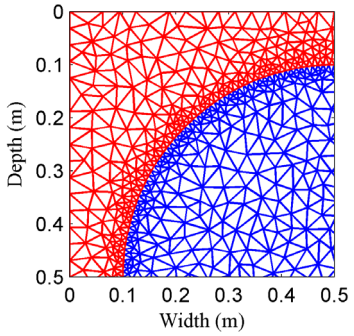

Figure 1. Numerical mesh used for the 2D simulation. A quarter of the sample domain is shown. Blue and red lines distinguish elements with different material properties.

Methodology of the numerical creep test

We perform numerical modeling of a creep test to compute the time-dependent strain response to a compressive stress applied on the boundaries of a numerical rock sample, representing a partially saturated rock (White, 1975; White et al., 1975). Then we use the time-dependent stress-strain relation to calculate attenuation and velocity dispersion due to fluid flow, according to Masson and Pride (2007).

In the 1D White's model, a partially saturated rock is represented by a poroelastic solid composed of two periodically alternating layers, each one fully saturated by a different fluid. The minimum Representative Volume Element (RVE) in this case contains one pair of layers with different fluid content. We refer as RVE to the smallest sample that statistically represents the distribution of heterogeneities in the rock. The numerical rock sample for our simulation is simply the mentioned RVE. We consider that the relative fluid velocity is zero on the boundaries (undrained condition). Due to symmetry reasons (the fluid flow is zero in the middle of the layers during the experiment), the numerical rock sample is selected from the layered medium as half a layer on top and bottom, and one layer in the middle. We simulate a 1D compression test by applying a step load only at the top of the sample and setting the displacement at the bottom to zero. We use variable time steps, with small time increments at the beginning of the simulation, and larger time increments towards the end. During the simulation, the stress and strain rates are calculated and volumetrically averaged over the sample domain. Next, a discrete Fourier transform is applied to the averaged stress and strain rates to obtain their

values as functions of frequency, f. The frequency-dependent quality factor and phase velocity are then calculated from the averaged stress and strain rates, according to Masson and Pride, 2007.

In 2D, the partially saturated rock can be represented by a poroelastic solid fully saturated with one fluid, with circular inclusions of the same solid material fully saturated by another fluid. Our numerical rock sample is the RVE, selected as a square with one circular inclusion in the middle. The boundary of the square corresponds, approximately, to the region where the fluid flow is zero. We simulate a 2D pure compression test by applying compressive step loads of equal magnitude on the four boundaries of the square sample.

Numerical tests

We test the 1D algorithm for a fractured rock described as a layered model in which the fractures are very thin (5 mm) compliant layers alternating with much thicker (5 m) layers of a stiffer porous rock of lower porosity and permeability (Table 2). We assume the thicker layers to be saturated with water and the fractures with gas (Table 3), because the wetting fluid (the water) preferentially saturates regions of small pores due to capillary effects (Goertz and Knight, 1998). For the simulation, the thin layer is divided into 20 elements and the thick layer into 400 elements. The total simulated time is 7.4 s, divided into 200 time increments of variable length. The simulation lasts less than two seconds on a personal computer. Figure 2 shows the numerical and analytical (e.g., Carcione and Picotti, 2006) results for the phase velocity, V_p, and the inverse of quality factor, $1/Q$. The differences in thickness and petrophysical parameters have a significant effect on a broad range of frequencies, but the numerical results fit well the analytical solution.

Table 2. Petrophysical parameters for the fractured rock.

Rock matrix	Surrounding rock	Fractures
h (m)	5	0.005
k (mD)	100	1000
ϕ	0.10	0.20
μ (GPa)	5	3
K (GPa)	6	4
K_s (GPa)	40	40
ρ_s (kg/m^3)	2700	2700

Table 3. Petrophysical parameters for water and gas.

Fluid	Water	Gas
$\boldsymbol{K}_f$ (GPa)	2.3	0.022
ρ_f (kg/m^3)	1000	140
η (Pa s)	0.003	10^{-5}

The 2D algorithm is tested for gas-saturated sandstone with circular water-saturated inclusions (Tables 3 and 4). The side of the square is 1 m and the radius of the inclusion is 40 cm. We use a total time of 0.39 s, divided into 200 time increments of variable length. The spatial domain contains approximately 1200 triangular elements of variable area (Figure 1), yielding higher resolution close to the boundary of the inclusion where most of the fluid flow occurs. The numerical results (Figure 3) for the real part of the undrained bulk modulus, K_u, and the inverse of the quality factor associated with a pure undrained compression, $1/Q_{Ku}$, are checked against theoretical low- and high-frequency limits (e.g., Toms et al., 2006).

Table 4. Petrophysical parameters for a sandstone.

Rock matrix	Sandstone
k (mD)	100
ϕ	0.20
μ (GPa)	3
K (GPa)	4
K_s (GPa)	40
ρ_s (kg/m^3)	2700

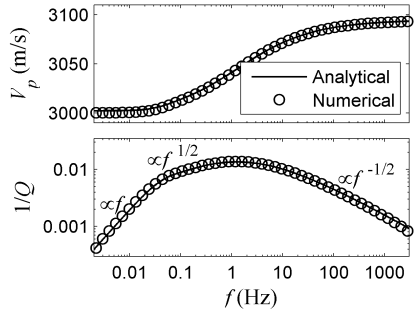

Figure 2. Result of the 1D simulation for the fractured rock.

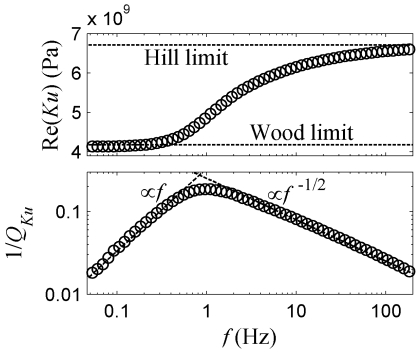

Figure 3. Result of the 2D simulation for gas-saturated sandstone with circular water-saturated inclusions.

Rocks with random distribution of saturation

We numerically investigate the effect of a random size distribution of saturation heterogeneities on the frequency-dependent attenuation and phase velocity of a rock. The

model is a layered medium consisting of one hundred pairs of layers of homogeneous solid frame, each pair composed of a fully gas-saturated layer at the top and a fully water-saturated layer at the bottom (Table 3 and 4). We build up the model by generating one hundred thicknesses of pairs randomly varying from 1 cm to 1 m, and one hundred gas saturation values for such pairs randomly varying from 10 to 90 % (Figure 4). The random values are generated with the function *rand* from MATLAB. The overall gas saturation in the model is 46.4 %. The minimum and maximum thicknesses are 0.15 and 70 cm for gas-saturated layers, and 0.43 and 81 cm for water-saturated layers. The model thickness is 44.9 m, and the numerical rock sample is the entire model. Layers with thicknesses lower than 5 cm are divided into 20 elements, the ones from 5 to 50 cm, into 40 elements, and the ones larger than 50 cm, into 60 elements. The total simulated time is 9.2 s, divided into 200 increments with variable length. The simulation lasts less than one minute on a personal computer. Figure 5 shows the numerical solution, and an approximate analytical solution calculated with a volume average of the analytical solutions of the 1D White's model (e.g., Carcione and Picotti, 2006) for the P-wave modulus of each pair:

$$H_{avg} \approx \left(\sum_{n=1}^{100} L_n H_n \right) \Big/ \sum_{n=1}^{100} L_n , \qquad (5)$$

where L_n is the thickness of the n-th pair of layers having the complex P-wave modulus H_n. The approximated P-wave modulus, H_{avg}, is used to calculate $1/Q$ and V_p (e.g., Carcione, 2007). We observe in Figure 5 that the low-frequency asymptote of $1/Q$ has the theoretically predicted behavior for finite random media (Müller and Rothert, 2006), i.e., proportional to frequency. The approximated analytical results fit well the correct numerical results.

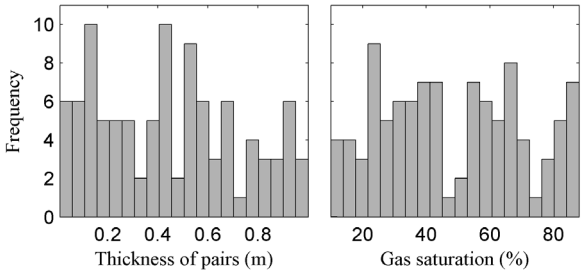

Figure 4. Frequency distribution of (left) thicknesses of the one hundred pairs of gas- and water-saturated layers and (right) values of gas saturation in those pairs.

Conclusions

We presented a finite element scheme to calculate frequency-dependent attenuation and velocity dispersion in the seismic frequency range due to fluid flow in poroelastic rocks with mesoscopic-scale heterogeneities using a quasi-static creep test. The methodology for the creep test is based on work presented by Masson and Pride (2007), but instead of solving Biot's equations of wave propagation in porous media (Biot, 1962) using the finite difference method, we solve Biot's equations of consolidation (Biot, 1941) using the finite element method. The numerical scheme employs natural boundary conditions for no fluid flow to represent an undrained rock sample. The time derivatives are implicitly solved, allowing for large and variable time increments and making the algorithm computationally efficient. Comparisons with analytical solutions show that our 1D and 2D numerical results are accurate over a wide range of frequencies. The numerical scheme is well-suited for modeling seismic attenuation and dispersion due to fluid flow in realistic media, such as 3D rock samples with heterogeneities of complicated geometries and arbitrary distribution patterns, or saturated by several fluid types (e.g., water, gas and oil).

We applied the numerical scheme to a rock with a random distribution of saturation. We proposed a volume average of analytical solution for approximating the complex P-wave modulus of such rocks. The approximated analytical solution fits well the correct numerical results. When well logging data are available, this average procedure can be directly used to estimate the frequency-dependent quality factor and velocity dispersion of a finite rock unit.

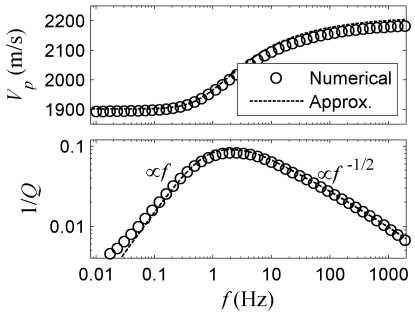

Figure 5. Numerical result for the layered model with random distribution of saturation and our approximated analytical solution.

Acknowledgments

This work has been supported by the ETH Zurich, the Swiss Innovation Promotion Agency (KTI/CTI) and Spectraseis. Beatriz Quintal thanks Yolanda Deubelbeiss, Yuri Podladchikov, Erik Saenger, and Marc Lambert for very constructive suggestions and input to this work.

EDITED REFERENCES

Note: This reference list is a copy-edited version of the reference list submitted by the author. Reference lists for the 2010 SEG Technical Program Expanded Abstracts have been copy edited so that references provided with the online metadata for each paper will achieve a high degree of linking to cited sources that appear on the Web.

REFERENCES

Biot, M. A., 1941, General theory of three-dimensional consolidation: Journal of Applied Physics, **12**, no. 2, 155–164, doi:10.1063/1.1712886.

Biot, M. A., 1962, Mechanics of deformation and acoustic propagation in porous media : Journal of Applied Physics, **33**, no. 4, 1482–1498, doi:10.1063/1.1728759.

Carcione, J. M., 2007, Wave Fields in Real Media: Theory and numerical simulation of wave propagation in anisotropic, anelastic, porous and electromagnetic media: Elsevier.

Carcione, J. M., and S. Picotti, 2006, P-wave seismic attenuation by slow-wave diffusion: Effects of inhomogeneous rock properties: Geophysics, **71**, no. 3, O1–O8, doi:10.1190/1.2194512.

Chapman, M., E. Liu, and X. Li, 2006, The influence of fluid-sensitive dispersion and attenuation on AVO analysis: Geophysical Journal International, **167**, no. 1, 89–105, doi:10.1111/j.1365-246X.2006.02919.x.

Dasgupta, R., and R. A. Clark, 1998, Estimation of Q from surface seismic reflection data: Geophysics, **63**, 2120–2128, doi:10.1190/1.1444505.

Dutta, N. C., and H. Odé, 1979a, Attenuation and dispersion of compressional waves in fluid filled porous rocks with partial gas saturation (White model) – Part I: Biot Theory: Geophysics, **44**, 1777–1788, doi:10.1190/1.1440938.

Dutta, N. C., and H. Odé, 1979b, Attenuation and dispersion of compressional waves in fluid filled porous rocks with partial gas saturation (White model) – Part II: Results: Geophysics, **44**, 1789–1805, doi:10.1190/1.1440939.

Frehner, M., S. M. Schmalholz, E. H. Saenger, and H. Steeb, 2008, Comparison of finite difference and finite element methods for simulating two-dimensional scattering of elastic waves: Physics of the Earth and Planetary Interiors, **171**, no. 1-4, 112–121, doi:10.1016/j.pepi.2008.07.003.

Goertz, D., and R. Knight, 1998, Elastic wave velocities during evaporative drying: Geophysics, **63**, 171–183, doi:10.1190/1.1444310.

Goloshubin, G., C. Van Shuyver, V. Korneev, D. Silin, and V. Vingalov, 2006, Reservoir imaging using low frequencies of seismic reflections: The Leading Edge, **25**, no. 5, 527–531, doi:10.1190/1.2202652.

Gurevich, B., and S. L. Lopatnikov, 1995, Velocity and attenuation of elastic waves in finely layered porous rocks: Geophysical Journal International, **121**, no. 3, 933–947, doi:10.1111/j.1365-246X.1995.tb06449.x.

Johnson, D. L., 2001, Theory of frequency dependent acoustics in patchy-saturated porous media : The Journal of the Acoustical Society of America, **110**, no. 2, 682–694, doi:10.1121/1.1381021.

Korneev, V. A., G. M. Goloshubin, T. M. Daley, and D. B. Silin, 2004, Seismic low-frequency effects in monitoring fluid-saturated reservoirs: Geophysics, **69**, 522–532, doi:10.1190/1.1707072.

Masson, Y. J., and S. R. Pride, 2007, Poroelastic finite difference modeling of seismic attenuation and dispersion due to mesoscopic-scale heterogeneity: Journal of Geophysical Research, **112**, B3, B03204, doi:10.1029/2006JB004592.

Müller, T. M., and B. Gurevich, 2005, Wave-induced fluid flow in random porous media: attenuation and dispersion of elastic waves: The Journal of the Acoustical Society of America, **117**, no. 5, 2732–2741, doi:10.1121/1.1894792. PubMed

Müller, T. M., and E. Rothert, 2006, Seismic attenuation due to wave-induced flow: Why Q in random structures scales differently: Geophysical Research Letters, **33**, no. 16, L16305, doi:10.1029/2006GL026789.

Norris, A. N., 1993, Low-frequency dispersion and attenuation in partially saturated rocks: The Journal of the Acoustical Society of America, **94**, no. 1, 359–370, doi:10.1121/1.407101.

Pride, S. R., and J. G. Berryman, 2003a, Linear dynamics of double-porosity and dual-permeability materials. I. Governing Equations and acoustic attenuation: Physical Review E: Statistical, Nonlinear, and Soft Matter Physics, **68**, no. 3, 036603, doi:10.1103/PhysRevE.68.036603.

Pride, S. R., and J. G. Berryman, 2003b, Linear dynamics of double-porosity and dual-permeability materials. II. Fluid transport equations: Physical Review E: Statistical, Nonlinear, and Soft Matter Physics, **68**, doi: 10.1103/PhysRevE.68.036603.

Quintal, B., S. M. Schmalholz, and Y. Y. Podladchikov, 2009, Low-frequency reflections from a thin layer with high attenuation caused by interlayer flow: Geophysics, **74**, no. 15, N23.

Rapoport, M. B., L. I. Rapoport, and V. I. Ryjkov, 2004, Direct detection of oil and gas fields based on seismic inelasticity effect: The Leading Edge, **23**, no. 3, 276–278, doi:10.1190/1.1690901.

Shewchuk, J. R., 1996, Triangle: Engineering a 2D quality mesh generator and Delaunay triangulator, in C. L. Ming and M. Dinesh, eds., Applied computation geometry: Towards geometric engineering: Springer Verlag Lecture Notes in Computer Science 1148, 203-222.

Shewchuk, J. R., 2002, Delaunay refinement algorithms for triangular mesh generation: Computational Geometry, **22**, no. 1-3, 21–74, doi:10.1016/S0925-7721(01)00047-5.

Toms, J., T. M. Muller, R. Ciz, and B. Gurevich, 2006, Comparative review of theoretical models for elastic wave attenuation and dispersion in partially saturated rocks: Soil Dynamics and Earthquake Engineering, **26**, no. 6-7, 548–565, doi:10.1016/j.soildyn.2006.01.008.

White, J. E., 1975, Computed seismic speeds and attenuation in rocks with partial gas saturation: Geophysics, **40**, 224–232, doi:10.1190/1.1440520.

White, J. E., N. G. Mikhaylova, and F. M. Lyakhovitskiy, 1975, Low-frequency seismic waves in fluid saturated layered rocks: Izvestiya, Academy of Sciences, USSR. Physics of the Solid Earth, **11**, 654–659.

Zhu, X., and G. A. McMechan, 1991, Numerical simulation of seismic responses of poroelastic reservoirs using Biot theory: Geophysics, **56**, 328–339, doi:10.1190/1.1443047.

Zienkiewicz, O. C., and R. L. Taylor, 1989, The finite element method, Vol. 1: McGraw Hill.

Zienkiewicz, O. C., and T. Shiomi, 1984, Dynamical behavior of saturated porous media; The generalized Biot formulation and its numerical solution: International Journal for Numerical and Analytical Methods in Geomechanics, **8**, no. 1, 71–96, doi:10.1002/nag.1610080106.